Data in brief 24 (2019) 103922

Contents lists available at ScienceDirect

Data in brief

journal homepage: www.elsevier.com/locate/dib

Data Article

Data on laser induced preferential crystal (re) orientation by picosecond laser ablation of zinc in air

H. Mustafa [a, *], M.P. Aarnts [b], L. Capuano [a], D.T.A. Matthews [a, b, c], G.R.B.E. Römer [a]

[a] Chair of Laser Processing, Department of Mechanics of Solids, Surfaces & Systems (MS^3), Faculty of Engineering Technology, University of Twente, Enschede, the Netherlands
[b] Research & Development, Tata Steel, PO Box 10000, 1970 CA IJmuiden, the Netherlands
[c] Chair of Skin Tribology, Department of Mechanics of Solids, Surfaces & Systems (MS^3), Faculty of Engineering Technology, University of Twente, Enschede, the Netherlands

ARTICLE INFO

Article history:
Received 1 March 2019
Received in revised form 6 April 2019
Accepted 8 April 2019
Available online 15 April 2019

Keywords:
Picosecond laser
Polycrystalline zinc
Galvanized steel
Laser induced preferential crystal orientation
Laser ablation

ABSTRACT

Laser ablation of zinc is performed with a 6.7 ps pulsed laser source to investigate the ablation mechanism and resulting morphology of the irradiated surface. The data shows the changes in crater morphology, as well as chemical composition, for different number of pulses and laser fluence levels. We observed Laser Induced Preferential Crystal Orientation (LIPCO), as a result of ultra-short pulsed laser processing of Zn at a wavelength of 515 nm. Crystallographic data for other laser wavelengths, namely 343 and 1030 nm, as well as for Zn coated steel are also provided in support of this observation. Data presented in this article are related to the research article "Investigation of the ultrashort pulsed laser processing of zinc at 515 nm: morphology, crystallography and ablation threshold" [1].

DOI of original article: https://doi.org/10.1016/j.matdes.2019.107675.
* Corresponding author.
E-mail address: h.mustafa@utwente.nl (H. Mustafa).

https://doi.org/10.1016/j.dib.2019.103922

Specifications table

Subject area	*Material Science Engineering*
More specific subject area	*Laser Material Processing*
Type of data	*Figures*
How data was acquired	*CLSM (Keyence VK-9700), SEM (Jeol JSM-7200F), XPS (Physical Electronics Quantera SXM), EBSD (Oxford Instruments Nordlys II)*
Data format	*Raw and analyzed/processed*
Experimental factors	*Mechanical polishing of pure Zn samples and chemical cleaning of galvanized steel samples.*
Experimental features	*Effects of laser processing parameters on the morphology, chemical composition and crystallographic orientation of Zn and Zn coated steel are demonstrated via processed confocal microscopy data as well as raw EBSD data.*
Data source location	*Chair of Laser Processing, Department of Mechanics of Solids, Surfaces & Systems (MS3), Faculty of Engineering Technology, University of Twente, Enschede, the Netherlands*
Data accessibility	*Data are provided with this article*
Related research article	*H. Mustafa, D. T. A. Matthews, G. R. B. E. Römer, Investigation of the ultrashort pulsed laser processing of zinc at* 515 nm*: morphology, crystallography and ablation threshold, Materials & Design 169 (2019) 107675–107687* [1]

Value of the data

- Data shows the changes in surface morphology of laser ablated craters on polished Zn at a wavelength of 515 nm for a laser pulse duration of 6.7 ps, and various number of laser pulses and laser fluence levels.
- The presented data may be used to compare the chemical compositional changes during intense laser pulse irradiation of Zn.
- The dataset will be useful for further investigation on the Laser Induced Preferential Crystal Orientation (LIPCO) in Zn and Zn coated products.

1. Data

1.1. Crater morphology

The degree of micro- and nano-particle deposition around a given crater is found to qualitatively increase with increasing ablated depth. Fig. 1 shows representative craters at all the experimental conditions. The yellow line separates the craters around which remarkable particle redeposition occurs, while the blue line demarcates the craters that show a so-called “drilling effect”. In the context of this work, when the ratio between the depth and the diameter of the crater hcrater/Dcrater $\geq$0.2 and the ratio of crater diameter to beam diameter Dcrater/2ω0 $\geq$ 1.5, the crater morphology is said to demonstrate this drilling effect. Also in this case, the maximum depth of the craters is greater than 8.5 μm. This is shown in Fig. 2 with the dashed horizontal line. The solid horizontal line at 4 μm represents the depth above which micrometric particle redeposition becomes prominent.

1.2. Chemical composition

Both EDS and XPS measurements have been performed on laser-induced craters. However, no significant difference in the chemical composition of Zn, Al, C and O was observed. For XPS measurements, the average carbon concentration for all laser processing conditions is approximately 50%, with C1s binding energy of 284.8 eV, which is attributed to adventitious carbon [2]. Fig. 3 shows the elementwise concentration of Zn, Al and O by offsetting the C concentration. In this figure, the graph on the left is for $F_0 = 2.4$ J/cm^2 for number of pulses ranging from $N = 1$ to 50, while the graph on the right shows the atomic concentration for single pulse ($N = 1$) at fluence levels up to 35 J/cm^2.

1.3. Crystallography

For Zn, laser induced preferential crystal orientation (LIPCO) is not limited to the laser wavelength of 515 nm, for picosecond laser pulses. Similar reorientation of the modified area was also observed for

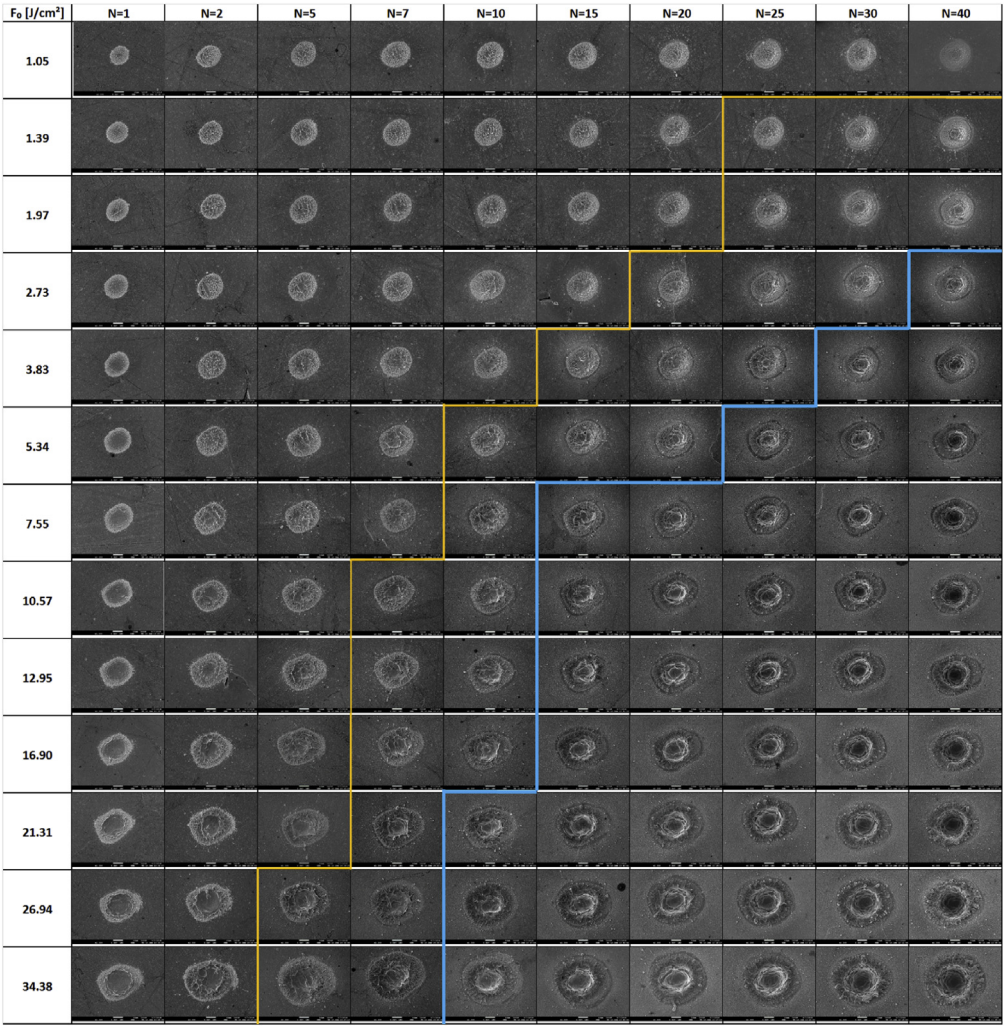

Fig. 1. SEM micrographs (top view) of zinc surface irradiated at different laser peak fluence F_0 [J/cm^2] levels (rows) and at different number of laser pulses N (columns). Yellow and blue lines mark the regions with prominent micrometric droplets around the crater and drilling effect respectively. All images are in the same scale, where the white scale bar indicates 10 μm.

laser wavelengths of 1030 and 343 nm as shown in Fig. 4. This suggests that this physical phenomenon does not strongly depend on laser wavelength. However, (so long as the irradiated grain is not already in the preferred orientation), for 1030 nm, partial (preferential) re-orientation is found, whereas for wavelengths of 515 and 343 nm full reorientation is observed, which can be seen in Fig. 4. It appears that the flatter the crater bottom gets by melt expulsion, the higher the degree of preferred orientation is observed. More details of LIPCO and proposed physical driving mechanism are discussed in Ref. [1].

Crystal (re)orientation, i.e. re-orientating from any crystallographic plane to (wards) ⟨0001⟩, was also observed for Zn coated steel (i.e. galvanized steel) processed at a wavelength of 515 nm as shown

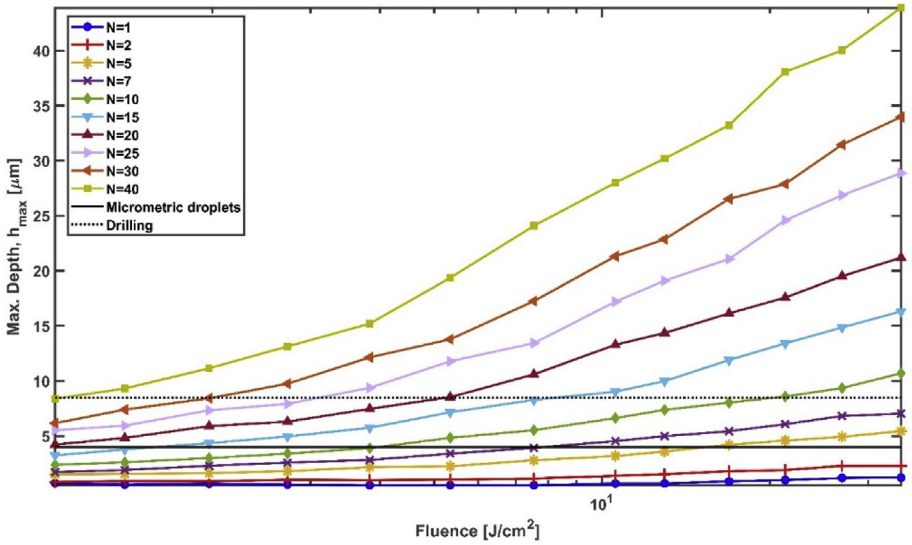

Fig. 2. Maximum depth of the ablated craters as a function of peak fluence F_0 for different number of pulses N.

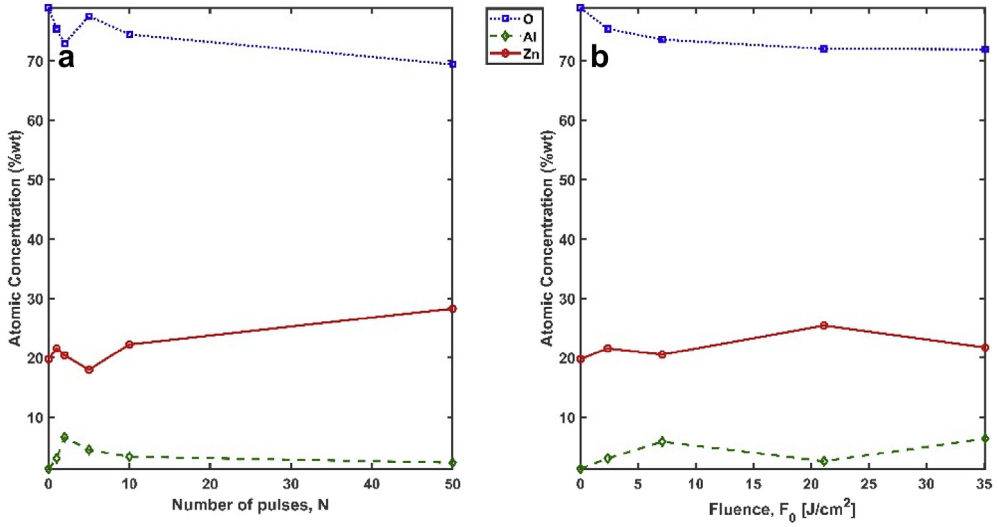

Fig. 3. Atomic concentration of Zn, Al and O, (a) for different number of pulses, N at $F_0 = 2.4$ J/cm^2, and (b) for different fluence levels, F_0 at $N = 1$.

in Fig. 5(b). However, we did not observe this phenomenon (LIPCO) for craters produced with a wavelength of 1030 nm (see Fig. 5(a)). At this wavelength, it is difficult to observe LIPCO, because of the surface roughness (non-indexed points [3]) and crater depth (shadowing effect [4]). Moreover, the surface chemical composition of galvanized steel is different than pure Zn due to the presence of an Al rich oxide film, which results from precipitation during the hot dip galvanizing process [5]. Therefore,

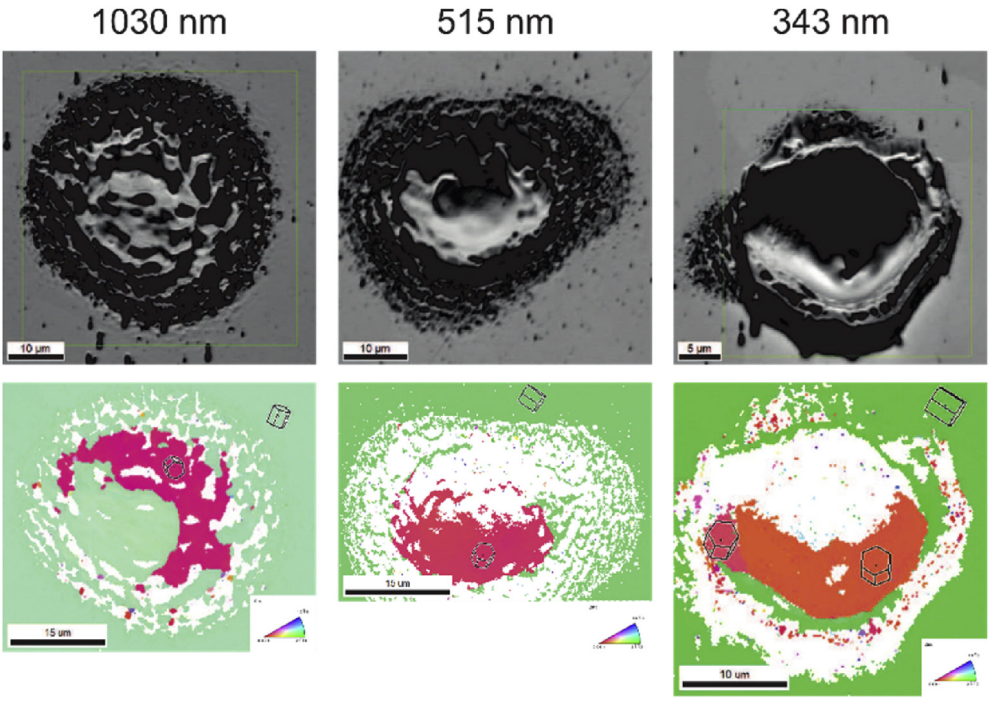

Fig. 4. SEM image and EBSD mapping of zinc orientation with corresponding crystal shape at different laser wavelengths. Insets in the EBSD images show the inverse pole figures.

slight differences in surface chemistry or stress in the Zn crystals might also have an influence on the degree of crystal (re)orientation. In any case, more research is required to study whether LIPCO also occurs (to which extend, or not) at other wavelength, other laser-conditions and for other Zn-based alloys.

2. Experimental design, materials and methods

Laser ablation experiments were performed in a similar manner as mentioned in Ref. [1]. Along with the second harmonic wavelength, the fundamental (1030 nm) and the third harmonic (343 nm) wavelengths were also used in this work. The focal spot (1/e2) radius ω_0 were measured using is a MicroSpot Monitor (Primes GmbH, Germany) and found to equal 14.4 ± 1.6 µm, 11.9 ± 1.6 µm and 7.4 ± 0.5 µm with an ellipticity 0.93, 0.78 and 0.86 for a wavelength of 1030, 515 and 343 nm respectively.

Pure zinc samples were similar to those mentioned in Ref. [1]. The coated samples (galvanized steel) with a surface roughness (S_a) of 0.3 µm is commercially produced according to European standard EN10346:2015 and has a nominal Zn layer thickness of 10 µm. While pure zinc samples were cleaned with ethanol in an ultrasonic bath, the coated samples were cleaned (swabbing) using Ammonia (<5%) solution prior to and after the ablation experiments.

The dimensional, morphological and crystallographic measurements using confocal laser scanning microscope (CLSM), scanning electron microscope (SEM) and electron backscatter diffraction (EBSD) respectively, were performed as mentioned in Ref. [1]. X-ray Photoelectron Spectroscopy (XPS), (Quantera SXM of Physical Electronics, USA) was used to analyze the chemical composition of the pure Zn samples at similar conditions mentioned in Ref. [6].

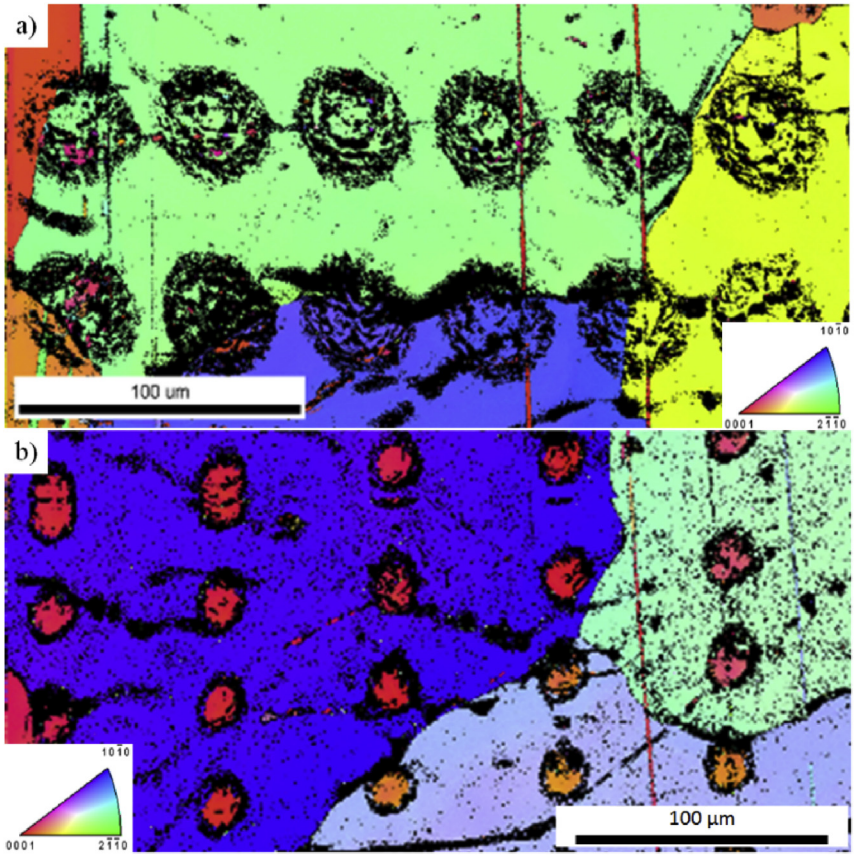

Fig. 5. EBSD Mapping of zinc orientation of picosecond pulsed laser induced craters on galvanized steel processed with N = 1 at a wavelength of (a) 1030 nm with F_0 = 40 J/cm^2, and (b) 515 nm with F_0 = 30 J/cm^2. Inset shows the inverse pole figure.

Acknowledgements

The authors would like to acknowledge the financial support of Tata Steel Nederland Technology BV. We would also like to thank G. Kip of MESA+, University of Twente for his help with the XPS measurements.

Transparency document

Transparency document associated with this article can be found in the online version at https://doi.org/10.1016/j.dib.2019.103922.

References

[1] H. Mustafa, D.T.A. Matthews, G.R.B.E. Römer, Investigation of the ultrashort pulsed laser processing of zinc at 515 nm: morphology, crystallography and ablation threshold, Mater. Des. 169 (2019) 107675–107687.
[2] S. Evans, Correction for the effects of adventitious carbon overlayers in quantitative XPS analysis, Surf. Interface Anal. Int. J. Devoted Develop. Appl. Tech. Anal. Surf. Interfaces Thin Films 25 (1997) 924–930.
[3] L.V. Saraf, Dependence of the electron beam energy and types of surface to determine EBSD indexing reliability in yttria-stabilized zirconia, Microsc. Microanal. 18 (2) (2012) 371–378.
[4] T.L. Matteson, S.W. Schwarz, E.C. Houge, B.W. Kempshall, L.A. Giannuzzi, Electron backscattering diffraction investigation of focused ion beam surfaces, J. Electron. Mater. 31 (1) (2002) 33–39.

[5] J.M. Mataigne, V. Vaché, M. Repoux, Surface chemistry and reactivity of skin-passed hot dip galvanized coating, Revue de Métallurgie–International Journal of Metallurgy 106 (1) (2009) 41–47.
[6] H. Mustafa, R. Pohl, T.C. Bor, B. Pathiraj, D.T.A. Matthews, G.R.B.E. Römer, Picosecond-pulsed laser ablation of zinc: crater morphology and comparison of methods to determine ablation threshold, Optic Express 26 (2018) 18664–18683.